J. Biomed. Eng. Res.
Vol.26, No.1, 55-63, 2005

3-D High Resolution Ultrasonic Transmission Tomography and Soft Tissue Differentiation

Tae-Seong Kim

Dept. of Biomedical Engineering, Kyung Hee University
(Received October 1, 2004. Accepted January 6, 2005)

Abstract: A novel imaging system for High-resolution Ultrasonic Transmission Tomography (HUTT) and soft tissue differentiation methodology for the HUTT system are presented. The critical innovation of the HUTT system includes the use of sub-millimeter transducer elements for both transmitter and receiver arrays and multi-band analysis of the first-arrival pulse. The first-arrival pulse is detected and extracted from the received signal (i.e., snippet) at each azimuthal and angular location of a mechanical tomographic scanner in transmission mode. Each extracted snippet is processed to yield a multi-spectral vector of attenuation values at multiple frequency bands. These vectors form a 3-D sinogram representing a multi-spectral augmentation of the conventional 2-D sinogram. A filtered backprojection algorithm is used to reconstruct a stack of multi-spectral images for each 2-D tomographic slice that allow tissue characterization. A novel methodology for soft tissue differentiation using spectral target detection is presented. The representative 2-D and 3-D HUTT images formed at various frequency bands demonstrate the high-resolution capability of the system. It is shown that spherical objects with diameter down to 0.3mm can be detected. In addition, the results of soft tissue differentiation and characterization demonstrate the feasibility of quantitative soft tissue analysis for possible detection of lesions or cancerous tissue.

Key words: Ultrasonic transmission tomography, Multi-spectral imaging, Soft tissue differentiation, Spectral target detection

INTRODUCTION

In the field of medical imaging, ultrasound has been utilized extensively, since it is considered safe due to non-ionizing radiation and rich in information content. Conventional pulse-echo ultrasound imaging systems provide mappings of tissue interfaces representative of acoustic impedance differences. These mappings constitute images depicting the geometry of tissue structures characterized by different acoustic impedance. However, the quantitative accuracy of imaging information in the echo-mode systems is compromised by the complex mechanisms of scattering in inhomogeneous and anisotropic media, such as living tissue. In order to enhance the amount and quality of extracted quantitative medical information, ultrasonic imaging in a transmission mode was conceived in conjunction with computerized tomography. In 1974, the first ultrasound computed tomography (UCT) system was reported by Greenleaf et al. [1]. Follow-up studies of the same group reported interesting results of 2-D images representing the distribution of acoustic attenuation and sound speed across the tomogram [2,3]. In 1977, Glover and Sharp reported UCT image reconstructions of 2-D sound speed distributions of simple phantoms such as beef liver and human breasts, demonstrating the potential of UCT for soft tissue imaging [4]. In 1978, Kak and Dines introduced various methods of measuring ultrasound attenuation in transmission-mode imaging [5]. The following year, Miller and his colleagues attempted tissue differentiation utilizing ultrasonic attenuation distributions, obtained via UCT, as quantitative indices for myocardial changes due to ischemia in the heart of dogs [6].

Based on these experimental studies, UCT was used to collect tomographic images from patients with breast cancer [7] and to establish initial criteria for distinguishing benign from malignant lesions in a preliminary clinical study [8]. Recently, improved UCT

This research was supported by the Kyung Hee University Research Fund in 2004 (KHU-20040450). The author is grateful to Drs. V. Z. Marmarelis and J. W. Jeong at the University of Southern California for providing partial data and helpful comments.
Corresponding Author: Tae-Seong Kim, Ph.D.
Dept. of Biomedical Engineering
College of Electronics and Informations
Kyung Hee University
1 Seochun, Kiheung, Yongin, Kyungki, 449-701
Tel. 031-201-3731
E-mail. tskim@khu.ac.kr

systems using transducer arrays have been reported as a new trend in medial ultrasonic imaging [9,10,11].

The main advantages of transmission-mode UCT imaging systems over conventional echo-mode imaging systems are: (1) they provide quantitative information; (2) the power in the transmitted (forward-scattered) signal is greater than the power in the reflected (back-scattered) signal for soft tissue structures where the refractive index is not far from unity; (3) the use of only the first-arrival pulse in transmission-mode systems alleviates multi-path problems that compromise imaging quality in echo-mode systems due to scattering in living tissue; and (4) they allow soft tissue differentiation based on quantitative information, rather than qualitative information of the conventional echo ultrasound.

Transmission-mode UCT imaging systems also exhibit the following advantages over X-ray medical imaging: (1) they use non-ionizing radiation and can be repeated many times; (2) they are capable of soft tissue differentiation; (3) they can generate 3-D images, instead of potentially obscured 2-D projection images generated by X-rays.

The main limitations of UCT imaging to date are: (1) limited resolution due to the size of transducers (2) the physics of nonlinear acoustic propagation in living tissue; (3) the relatively low scanning speed for clinically useful 3-D imaging applications.

However, with technical advancement in multi-channel electronics and transducer manufacturing, these limitations can be overcome. Toward the development of a clinically useful scanner, we have developed a 3-D high resolution ultrasonic transmission tomography (HUTT) system that has a scanning speed capability and high resolution such that it can be practically useful in clinical applications [12]. The HUTT system incorporates critical innovations of orthogonal triggering sequences and sub-millimeter transducer elements in large transmitter and receiver arrays, combined with advanced methods of signal processing (e.g., multi-band analysis in the Method section) of the first-arrival pulse.

Since the introduction of echo-based ultrasonic imaging, another challenge in diagnostic ultrasonic imaging has been soft tissue differentiation. Tremendous efforts have been made to differentiate soft biological tissues according to their acoustic parameters of tissues derived from scattered ultrasonic signals [13,14,15]. However, it has not been realized so far mainly due to the fundamental limitation: ultrasonic echo images do not provide quantitative information for reliable tissue characterization. Since soft tissue differentiation is a powerful potential of diagnostic ultrasonic imaging that can be used to differentiate lesions or cancerous tissue from normal tissue, it is critical to come up with means of tissue characterization and differentiation. In addition to high resolution images that can be achieved with the HUTT system, one significant outcome of transmission imaging is the quantitative information contained in the multi-spectral images that can be utilized for reliable tissue characterization.

This paper introduces the latest efforts in developing a high resolution tomographic imaging system using transmission ultrasound and discusses the technical limitations and challenges of developing such a system. Then novel soft tissue characterization and differentiation techniques that have been developed for the transmissive ultrasonic imaging system will be described. The results presented in this work demonstrate several advantages of transmissive ultrasonic imaging system through its potentials in obtaining 3-D high resolution images and performing soft tissue differentiation based on quantitative information in the tomographic images.

The following is the organization of this paper. In the Methods section, the transmission ultrasonic system is introduced with its technical innovations. Then multi-spectral image formation processes and soft tissue differentiation methods are described. In the Results section, the performance of the HUTT imaging system is demonstrated with representative 2-D and 3-D tomographic images of phantoms containing sub-millimeter and millimeter size particles. The previous studies [12, 20] had shown the detectability of spherical objects with their diameter down to 0.3mm and the feasibility of tissue differentiation for a single slice of several phantoms in 2-D. In this paper, the efficacy of the HUTT system is demonstrated with newly obtained 2-D and 3-D images of soft animal tissue and sheep kidney phantoms, revealing detailed anatomical structures and their sub-millimeter sub-structures. The quality of HUTT imagery is compared to high-resolution optical images and magnetic resonance images. Then based on the multi-band information of these images, the demonstrative results of soft tissue differentiation for multiple tomographic slices of inter- and intra-phantoms in 3-D are presented, proving the feasibility of the technique in more realistic settings. Finally further challenges and final remarks are given in the Discussion and Conclusion sections.

METHODS

High Resolution Ultrasonic Transmission Tomography

The mechanical scanning setup of the HUTT system is similar to X-ray computed tomography, employing azimuthal and angular scans using a pair of transmitting and receiving transducer elements as shown in Fig. 1.

The system is equipped with a pair of transmitting and receiving transducer arrays with element size of 0.4 mm x 0.4 mm, element pitch of 0.03 mm, 64 elements/probe, and center frequency of 8MHz for high-resolution imaging. The element size and center

frequency of the transducers are much smaller than the previously reported element size and higher than the previously reported range. A survey of UCT systems shows the range of the piezoelectric crystal size varies from 10 to 19mm and center frequency from 3.5 to 6.5MHz, as summarized in [12]. The tomographic scan is performed in parallel-beam transmission mode with a minimal azimuthal firing step of 0.4mm, a vertical elevation of 0.4mm, and angular step of 0.1 deg. Water is used to couple the transmitted and received acoustic waves with the imaged objects. The firing of transmitting transducers is achieved using custom-made pulsers which are individually triggered according to firing sequences.

To mitigate the effect of acoustic wave interference from multiple firing of transducers, each transducer is excited with its own firing sequence (e.g., 1 for firing and 0 for no firing), that is pseudo-orthogonal to other sequences, such that when a transducer fires, the others are maximally silent. Then to decode the received acoustic pulses at each transducer that is still vulnerable to multiple acoustic echoes and interference, the received signal is correlated with the firing sequence. At the maximum correlation, the corresponding portion of the forward scattered acoustic pulses are sampled at 100MHz and stored for signal averaging and multi-spectral analysis. The inevitable acoustic refraction effects at every interface between tissues, resulting in curved ultrasonic beam paths, were found to be very small for soft tissue imaging and can be ignored. Therefore, linear path is assumed as shown in Fig. 1 for each transmit-receive pair of transducers.

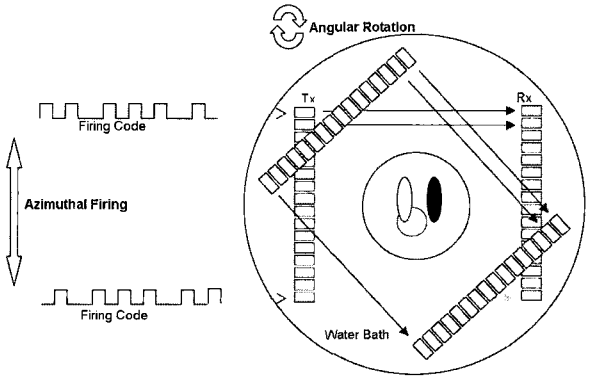

Fig. 1. Schematic scanning setup of the high resolution ultrasonic transmission tomography

Multi-band/Multi-spectral Imaging

In conventional UCT systems, time-of-flight (TOF) and attenuation (ATT) measurements were utilized in reconstructing images that convey acoustic information for each pixel of soft tissue in transmission mode. To extract the TOF and ATT imaging indices from the received signals, conventional UCT systems used maxima, minima, and zero-crossings in the received signals. However, previous studies showed that such measurements of TOF and ATT exhibit significant variations and systematic errors, mainly due to the frequency-dependent attenuation (scattering and absorption) that affects the wave shape of the received pulse [5,16].

In general, the frequency spectrum of the acoustic signal entering the objects is different from the spectrum of the forward-scattered output signal. This frequency-dependent attenuation has been often approximated by a power relationship in the range of 1~1.5 for soft tissue [5,17]. However, the frequency-dependent attenuation can be measured over the entire range of frequencies of interest, without constraining ourselves with a power relationship. The advantages of this approach are that no prior assumptions are required and greater flexibility is afforded for improved image reconstruction and tissue characterization by means of more acoustic parameters. For instance, attenuation values for multiple frequency-bands can be extracted for the vector characterization of each pixel, such as multi-spectral signatures of pixels.

In this study, such multi-band/multi-spectral attenuation values are derived by analyzing the first-arrival portion of the received pulse (termed "snippet"). In UCT, the first-arrival pulse is generally considered as a signal that has traveled the shorted path within an object, containing information most close to that of the linear path [2,4,5]. After averaging multiple pulses in the received signal according to the firing sequence, the first arrival pulse is detected and extracted from each averaged signal to avoid the multi-path problem. In general, a threshold above the ambient noise level is used in detection, but more sophisticated techniques such as matched filter or wavelet analysis can be used for improved detection. Typical water-only and object-through received signals sampled at 100MHz are shown in Figs. 2 (a) and (c) respectively, along with their detected and extracted first-arrival pulses superimposed on them with thick line. The respective power spectra are shown in the right column of Fig. 2.

To obtain frequency band specific characteristics from the first-arrival pulse, the magnitude of the FFT of the extracted snippet through soft tissues in Fig. 2 (d) is normalized by the FFT magnitude of a reference snippet corresponding to water-only conditions in Fig. 2 (b). Then logarithmic transformation of the ratio $A(f) = -\log\left|Y(f)/Y_w(f)\right|$, where $Y(f)$ is the FFT of the received snippet and $Y_w(f)$ is the FFT of the reference water-only snippet, yields projection data at each frequency band. This set of projection data represents a multi-band/multi-spectral vector characterization. The set of projection data or sinograms constitutes a 3-D augmentation of the

conventional 2-D sinogram. For each discrete frequency band f, the obtained sinogram $\{P_{i,j}(f)\}_z$ is composed of the $A(f)$ measurements at azimuthal position i, angular position j, and tomographic elevation z. To remove diffraction artifacts caused by acoustic scattering which results in striking artifacts in the reconstructed images, coherence enhancing nonlinear filtering is applied to each sinogram [18].

Each frequency-band attenuation sinogram yields a reconstructed image using a conventional filtered backprojection algorithm [19], resulting in a stack of images that represent a multi-band/multi-spectral 3-D augmentation of the 2-D conventional tomographic slice. This 3-D multi-spectral representation contains multi-band characteristics of individual pixel that can be used for tissue characterization/classification. Other acoustic attributes of the object (such as time-of-flight or wavelet decomposition coefficients) can also be obtained through appropriate snippet analysis.

It is clear that each reconstructed image at each frequency band f reveals different features of the object depending on its frequency-dependent characteristics since each multi-band sinogram contains the respective frequency-dependent acoustic attenuation of an imaged object. That is at given frequency bands, objects with their size comparable to the wavelength of given bands are resolved better. For instance, larger objects are better represented at lower frequency bands, and smaller objects are at the higher frequency bands.

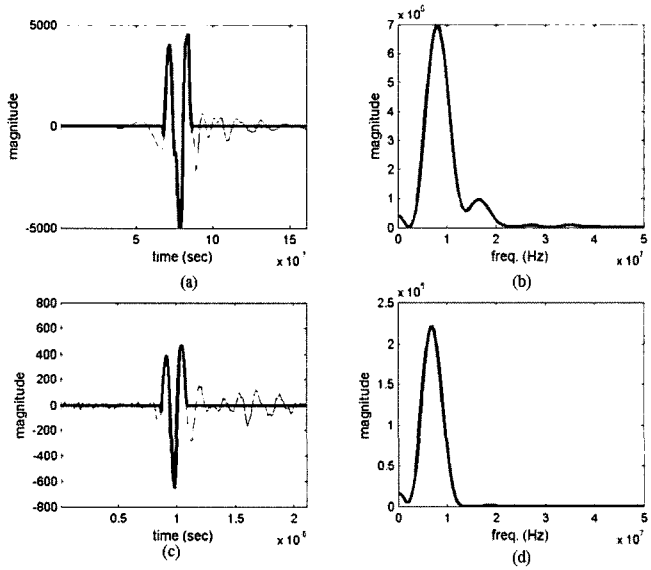

Fig. 2. Extracted first-arrival pulses (snippets) and their power spectral densities. The detected and extracted snippets (thick line) are superimposed on the received signals (thin line) as shown in (a) and (c) for water-only (top) and object-through (bottom) conditions. The power spectral density of each snippet is shown in (b) and (d).

Tissue Differentiation Using Multi-band Information

Soft tissue differentiation using multi-band information for ultrasonic transmission tomography was first proposed in [20]. Two different techniques were introduced: namely spectral unmixing and spectral target detection using constrained energy minimization (CEM). The initial results suggested higher sensitivity and specificity for the spectral target detection method. Also it was found to be more robust toward acoustic diffraction artifacts.

The CEM method has been widely used for target detection and classification in the hyperspectral imagery of remote sensing applications [21]. It can be easily implemented using only the knowledge about the target profile of interest and provides real-time process to identify the spectral profile matched with a given target. The concept of CEM is to build a spectral filter that minimizes the energy of the background pixels while enhancing the spectrum of the pixels that match the target spectrum. This filter f is given by:

$$f^T = \frac{s^T C_x^{-1}}{s^T C_x^{-1} s} \tag{1}$$

where s is the target spectrum, C_x is the correlation matrix of the background pixel spectra. Once the filter is designed, the "CEM score," y_j for each pixel j, is computed by the inner product between each pixel's spectrum, x_j and the filter:

$$y_j = f^T x_j . \tag{2}$$

Then, each CEM score map is thresholded according to statistical significance to get the binary detection map of the desired target tissue in the multi-band image.

The key features of the CEM are: (1) no linear mixture model is assumed for the pixels; (2) a gain is utilized to emphasize a given target signature (i.e., multi-spectral signature of target tissue) while minimizing other unknown target signatures; (3) *a priori* knowledge is required for the desired target spectral signatures, which must be obtained from controlled multi-band images; (4) a constraint is placed on the spectral signatures instead of the relative contributions; and (5) the computation of CEM is much faster than the constrained least-squares method (about 100 times), allowing tissue differentiation in real time.

RESULTS

High Resolution Ultrasound Transmission Imagery

In order to demonstrate the high-resolution capability of the HUTT system we have developed, various soft tissue-equivalent/animal tissue phantoms and whole animal kidneys were scanned. Some phantoms contained small objects (millimeter and sub-millimeter in size) mimicking micro-lesions in real tissues, since the system was designed for the early detection of malignant lesions (sub-mm in size) in breast cancer. Each phantom was scanned to get a 3-D stack of 2-D tomographic images (each in multi-band representation). In this section, a few sets of representative 2-D and 3-D imagery are presented.

Multi-band Imagery of Liver Phantom with Sub-mm Optical Fiber

To test the resolution capability of the HUTT system in real tissue, an animal tissue phantom was created by embedding 3 sub-millimeter (diameter of 0.56 mm) optical fibers in beef liver. The phantom was scanned with dx =0.4mm, $d\theta$ =1.0° up to 360 °. Figure 3 shows a set of three multi-band images, with the frequency band centered at 4.7MHz, 7.8MHz, and 9.4MHz respectively, of a tomographic slice of the liver phantom. The locations of the three optical fibers are indicated by the arrows and they are clearly discernible in the images. The three images also demonstrate the texture differences of liver in the different frequency bands for the same tomographic section. Clearly granular types of small objects are better differentiated in the image of higher frequency-band.

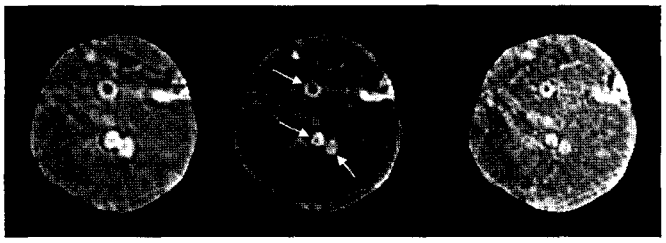

(a) 4.7MHz (b) 7.8MHz (c) 9.4MHz

Fig. 3. Multi-band images (center frequencies of 4.7MHz, 7.8MHz, and 9.4MHz) of a 2D tomographic section of a beef liver phantom with 3 optical fibers (diameter of 0.56mm) embedded in the liver. The arrows indicate the location of optical fibers. Note the texture difference of the liver images for the different frequency-bands.

Comparison of HUTT, MRI, and Optical Imagery of a Sheep Kidney Phantom

To test the resolution capability of the HUTT system in an inhomogeneous real tissue, a whole sheep kidney (approximate diameter of 4~5cm) was scanned. Figure 4 shows two sets of representative tomographic images of a sheep kidney phantom at the center frequency band of 6.25MHz and 9.38MHz. In the sagittal, coronal, and transaxial views of Fig. 4, internal structures of kidney, such as vessel- or duct-like structures are clearly visible at the boundaries of renal cortex and medulla.

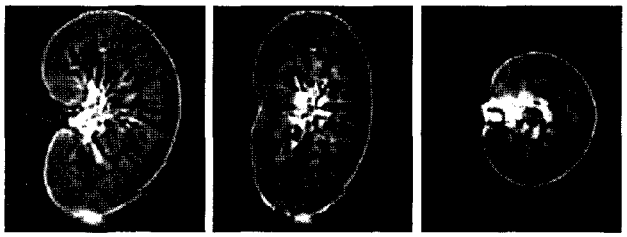

(a)

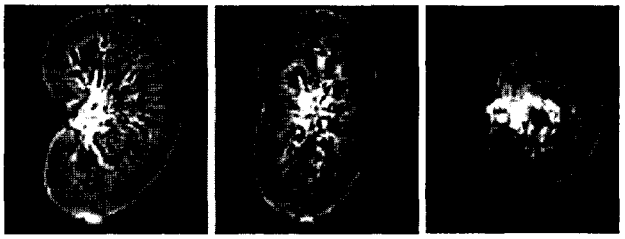

(b)

Fig. 4. Multi-band images of a sheep kidney at two different center frequency bands (a) 6.25 MHz and (b) 9.38 MHz

Figure 5 shows comparison of a HUTT image (dx =0.4mm; $d\theta$ =1.5°, 0° to 360 °; dz =0.8mm; FOV=8cm,) to its corresponding kidney slice images obtained through co-registration of image slices [22] acquired using MRI (TE=11; TR=566ms; Thickness = 1mm; FOV = 24cmx24cmx10cm; Matrix Size=256x256) and a digital camera (fine resolution approximately 0.025mmx0.025mm). Identical anatomical structures including renal cortex, medulla, tubule, calyx, and corpuscle, are clearly identifiable in all three images, but with better contrast and resolution in the HUTT images. The 3-D rendered fine inner vessel- or duct-like structures in Fig. 6 also demonstrate the 3-D resolution power of the HUTT system.

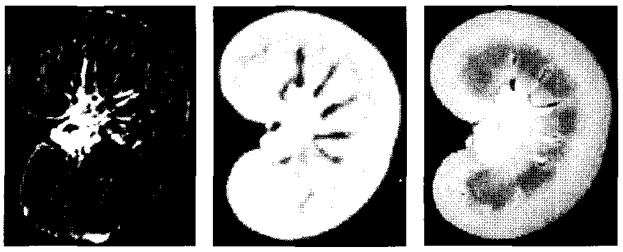

(a) (b) (c)

Fig. 5. Comparison of HUTT, MRI, and optical imagery of a sheep kidney (a) HUTT, (b) MRI, and (c) Optical image

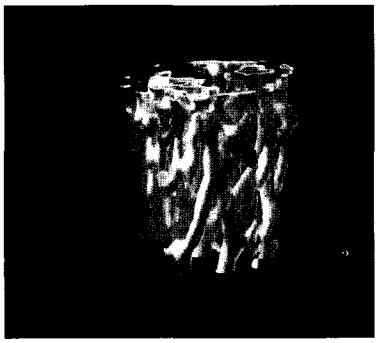

Fig. 6. 3D rendered kidney inner vessel- or duct-like structures

Soft Tissue Differentiation

In this section, the use of the multi-band "volume of information" resulting from the 3-D multi-spectral augmentation of each 2-D image slice to achieve tissue characterization through spectral target detection is demonstrated.

Animal-Tissue Phantom Study

In order to test the feasibility of differentiating soft biological tissues using multi-band information contained in multi-band images of the HUTT system, a new phantom was made in beef liver as a holding medium of three different animal tissues: pieces of chicken breast, pig fat, and beef kidney. The cross-sectional views of the phantom in three multi-band images are given in Fig. 7 (a). The obtained multi-band tomographic images at three different frequency bands are centered at 4.7MHz, 10.9MHz, and 15.6MHz respectively. The proposed target detection method using the CEM were applied on the multi-band images using the three target spectral signatures of the embedded tissue samples as shown in Fig. 7 (b). Figure 7 (c) shows the estimated relative contribution maps in gray-scale. Each map was converted to a binary mask by thresholding as shown in Fig. 7 (d) as white patches superimposed on the corresponding background images.

It is clearly shown that the target tissues can be detected (i.e., differentiated) from the background and other soft tissues if spectral profile for a target tissue is known. The implication of this is that once spectral profiles for cancerous tissues can be established, these cancerous tissues can be differentiated from multi-band images of the transmission ultrasonic system.

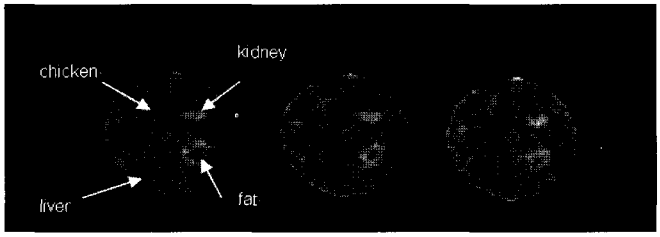

(a) Multi-band images at the center frequency of 4.7MHz, 10.9MHz, and 15.6MHz

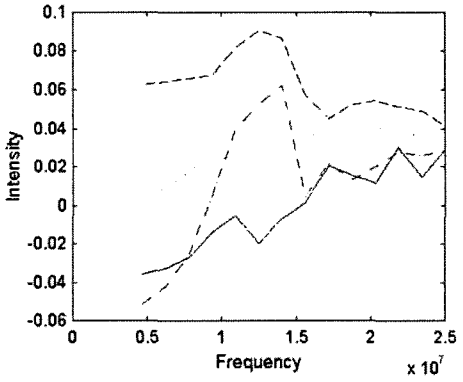

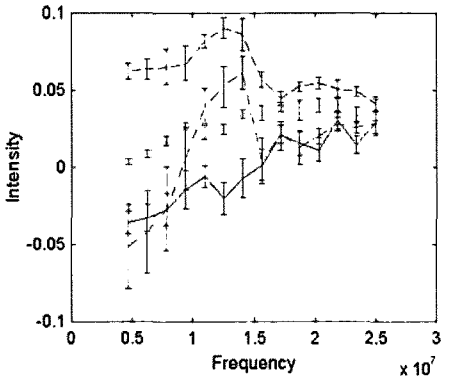

(b) Target spectral signatures of four different tissue types

(c) Score maps

(d) Differentiated and segmented tissues

Fig. 7. Soft tissue differentiation using spectral target detection method (a) Multi-band images, (b) Target spectral signatures of four different tissue types obtained from multi-band images without (left) and with (right) standard deviation bars: fat (-.) chicken (-), liver (...), and kidney (--), (c) The relative score maps in gray-scale, and (d) The thresholded binary masks (white regions) are superimposed on a multi-band image.

Soft Tissue Differentiation for Multiple Tomographic Slices

After validating the proposed tissue differentiation /characterization method with multi-band images of a *single* slice of several phantoms where spectral target profiles extracted, its feasibility for multi-band images of *multiple* tomographic slices was investigated. This step is essential to prove that representative spectral profiles can be used for tissue differentiation of different multiple tomographic slices of inter- and intra-objects.

In this study, phantoms were created with agar gel as an embedding medium for soft tissues such as fat and liver. The phantoms were scanned to yield multiple tomographic slices and their associated multi-band images. Then from multi-band images of a particular single tomographic slice, a set of representative spectral target profiles were extracted and used for tissue differentiation of entire tomographic slices of the phantoms.

Figure 9 (a) shows the cross-sectional views of the phantom and its transaxial view of the registered optical images. Target profiles of each tissue for this inter- and intra- phantom studies are given in Figs. 8 (a) and (b), revealing different patterns and variability. The profiles were applied to the CEM differentiator to detect the pixels of the entire phantom whose spectral profiles are similar to the corresponding target profile. The resulting clusters at the threshold of statistical significance $p=10^{-5}$ are shown in Figs. 9 (b) and (c). In these figures the white and gray colors indicate the cluster of liver and fat respectively. As shown in the coronal and sagittal views of Fig. 9 (b) and (c), the proposed method can isolate most pixels distributed in 3-D space into correct tissue types even though target profiles are obtained from a slice of the phantom. The similar results were produced with inter-phantom studies as well, proving that the spectral profile of each tissue type can be used to differentiate that particular tissue from inter- and intra-objects.

The results indicate that multi-band imaging provided by the HUTT system is reproducible without depending on the azimuth and elevation, and it results in enough robustness in the coherency of spectral profiles that can characterize the frequency dependent acoustic attenuation of particular tissue types.

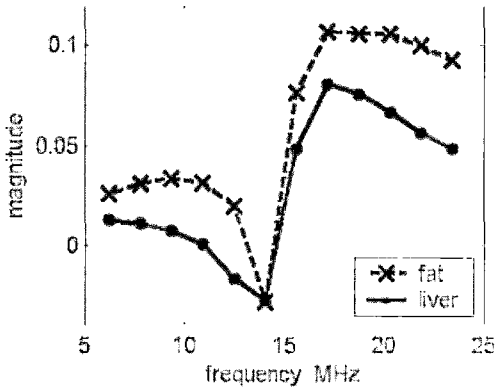

(a)

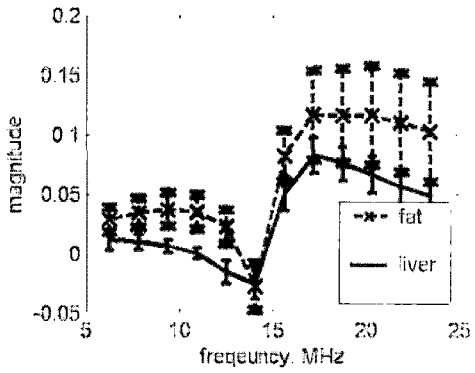

(b)

Fig. 8. Coherence of spectral profiles (a) Spectral patterns of two different tissues and (b) Spectral variability of two different tissues

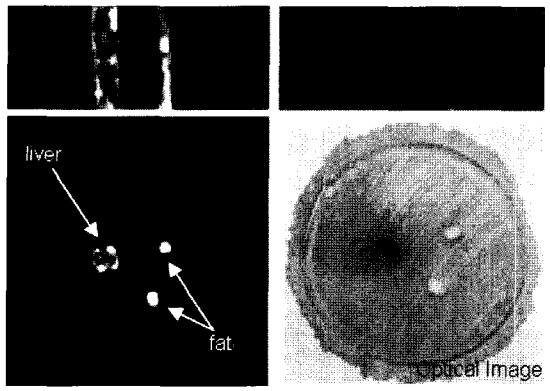

(a)

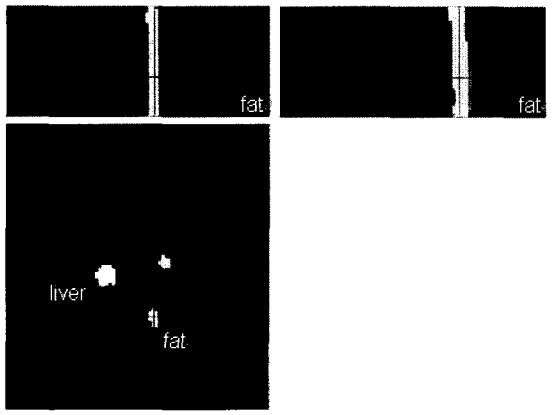

(b)

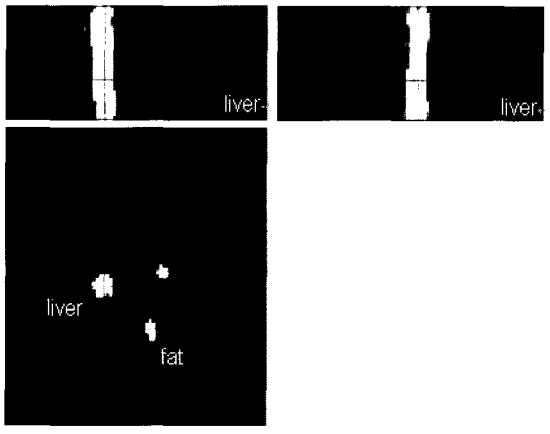

(c)

Fig. 9. The results of intra-phantom study (a) HUTT image and optical slice of the phantom: two pieces of fat and a piece of liver inside agar-gel, (b)-(c) Classification of fat (gray) and liver (white) tissues across multiple tomographic slices

DISCUSSION

The imaging results presented in this paper demonstrate the basic capability of the ultrasonic transmission imaging in producing high-resolution images and detecting sub-mm objects. These results are even extended to 3-D imaging of objects with similar resolution in the elevation direction. Furthermore, the tissue differentiation results demonstrate quantitative soft tissue characterization according to multi-band/multi-spectral profiles obtained from multi-band images of the HUTT system. Although it is the initial demonstration of transmission ultrasonic imaging, the demonstrated capability creates a host of exciting prospects for 3-D high resolution ultrasonic imaging of biological tissue and organs, and possible characterization of small tumors or other objects of clinical interest.

The remaining technical challenges in the imaging system development include (1) high-voltage pulsers that can handle fast pulsing of firing codes and optimal frequency transfer function characteristics as proposed in [23]; (2) large array of transducers with small enough crystal size and durability; (3) multi-channel receivers with fast enough sampling speed (>100MHz); (4) computing power for proper handling of multi-channel acoustic signals and image reconstruction. It is believed that technical advancement in multi-channel electronics and digital signal processing will overcome these challenges in the near future.

For tissue differentiation, further studies are underway to test the proposed methodology with in-vivo organs. Also to validate the technique in terms of specificity and sensitivity, the receiver operating characteristics (ROC) analysis is underway. Although the proposed technique, which utilizes spectral profiles of the HUTT multi-band images as a new feature set to classify or characterize soft tissues, is still in a beginning stage, the results look very promising and requires further investigation.

Despite the preliminary results presented in this work, it is strongly believed that the combination of quantitative transmission ultrasonic tomographic imaging and tissue differentiation methods could provide improved diagnostic or screening power for differentiation or detection of soft tissue lesions.

CONCLUSION

In this paper, the feasibility of high-resolution ultrasonic imaging is demonstrated using transmission ultrasound. Also based on the multi-band imaging capability of the ultrasonic transmission tomography, quantitative soft tissue differentiation methodology is introduced with its

feasibility demonstrated. Although the successful development of clinically-practical ultrasonic transmission system is not certain yet, its potential for improved clinical screening and diagnosis looks certain. Further investigation and development are underway to test the HUTT system for early screening and detection of breast cancer.

REFERENCES

[1] J. F. Greenleaf, S. A. Johnson, S. Lee, G. Herman, and E. Wood, in Acoustic Holography, N. Booth, Ed., pp. 591-603, Plenum, New York, 1974.

[2] J. F. Greenleaf, S. A. Johnson, R. C. Bahn, B. Rajagopalan, and S. Kenue, Introduction to computed ultrasound tomography, Computer Aided Tomography and Ultrasonics in Medicine, pp. 125-136, 1979.

[3] J. F. Greenleaf, and R. C. Bahn, *"Clinical Imaging with Transmissive Ultrasonic Computerized Tomography"*, IEEE Trans. Biomed. Engi., Vol. 28, No. 2, pp. 177-185, 1981.

[4] G. H. Glover, and J. C. Sharp, *"Reconstruction of Ultrasound Propagation Speed Distributions in Soft Tissue: Time-of-Flight Tomography"*, IEEE Trans. Sonics Ultrasonics, Vol. 24, No. 4, pp. 229-234, 1977.

[5] A. C. Kak, and K. A. Dines, *"Signal Processing of Broadband Pulsed Ultrasound: Measurement of Attenuation of Soft Biological Tissues"*, IEEE Trans. Biomed. Engi., Vol. 25, No. 4, pp. 321-344, 1978.

[6] J. G. Miller, J. R. Klepper, G. H. Brandenburger, L. J. Busse, M. O'Donnell, and J. W. Mimbs, Reconstructive Tomography based on Ultrasonic Attenuation, Computer Aided Tomography and Ultrasonics in Medicine, Raviv et al. (eds.), pp. 151-164, North-Holland Publishing Company, 1979.

[7] P. L. Carson, C. R. Meyer, A. L. Scherzinger, and T. V. Oughton, *"Breast Imaging in Coronal Planes with Simultaneous Pulse Echo and Transmission Ultrasound"*, Science, Vol. 214, No. 4, pp. 1141-1143, 1981.

[8] J. S. Schreiman, J. J. Gisvold, J. F. Greenleaf, and R. C. Bahn, *"Ultrasound Transmission Computed Tomography of the Breast"*, Radiology, 150, pp. 523-530, 1984.

[9] M. T. Nguyen, U. Faust, H. Bressmer, and P. Kugel, *"Ultrasound Tomography System Using Transmission and Reflection Mode with Electronic Scanning"*, IEEE Engi. Med. Bio. Soc., 14, pp. 2142-2143, 1992.

[10] R. Stotzka, J. Würfel, and T. O. Müller, *"Medical Imaging by Ultrasound-Computer Tomography"*, Proc. SPIE Medical Imaging, pp. 132, San Diego, 2002.

[11] S. G. Azevedo, T. L. Moore, R. D. Huber, S. W. Ferguson, R. L. Leach, and S. E. Benson, *"Apparatus for Circular Tomographic Ultrasound"*, Proc. SPIE Medical Imaging, pp. 131, San Diego, 2002.

V.Z. Marmarelis, T.-S. Kim, and R.E.N. Shehada, *"High Resolution Ultrasonic Transmission Tomography"*, Proc. SPIE Med. Imaging, Vol. 5035, pp. 33-40, 2003.

[12] L. Landini and L. Verrazzani, *"Spectral characterization of tissues microstructure by ultrasounds: a stochastic approach"*, IEEE Trans. Ultrason., Ferroelec., Freq Contr., Vol. 37, No. 5, pp. 448-456, 1990.

[13] *Decomposition and Compounding of Ultrasound Medical Images with Wavelet Packets"*, IEEE Trans. Med. Imaging, Vol. 20, No. 8, pp. 764-771, 2001.

[14] G. Georgiou, and F. S. Cohen, *"Tissue Characterization Using the Continuous Wavelet Transform"*, IEEE Trans. Ultrason., Ferroelec., Freq. Contr., Vol. 48, No. 2, pp. 355-363, 2001.

[15] K. A. Wear, *"The Effects of Frequency-Dependent Attenuation and Dispersion on Sound Speed Measurements: Applications in Human Trabecular Bone"*, IEEE Trans. Ultrason., Ferroelec., Freq. Contr., Vol. 47, No. 1, pp. 265-273, 2000.

[16] P. He, *"Acoustic parameter estimation based on attenuation and dispersion measurements"*, Proc. IEEE Eng. Med. Biol. Soc., Vol. 20, pp. 775-778, 1998.

[17] T.-S. Kim, C. Huang. J. Jeong, D. Shin, M. Singh, and V. Z. Marmarelis, *"Sinogram enhancement for ultrasonic transmission tomography using coherence enhancing diffusion"*, IEEE Int. Symposium on Ultrasonics, 1816-1819, 2003.

[18] G. N. Ramachandran, and A. V. Lakshminarayanan, *"Three-dimensional reconstruction from radiographs and electron micrographs: applications of convolutions instead of Fourier transforms"*, Proc. Nat. Acad. Sci. U.S., Vol. 68, No. 9, pp. 2236-2240, 1971.

[19] T.-S. Kim, S. Do, and V. Z. Marmarelis, *"Multi-band tissue differentiation in ultrasonic transmission tomography"*, Proc. SPIE Medical Imaging, Vol. 5035, pp. 41-48, 2003.

[20] C.-I. Chang, D. C. Heinz, *"Constrained Subpixel Target Detection for Remotely Sensed Imagery"*, IEEE Trans. Geosci. Remote Sensing, Vol. 38, No. 3, pp. 1144-1159, 2000.

[21] T.-S. Kim, M. Singh, W. Sungkarat, C. Zarow, and H. Chui, *"Automatic Reigstration of Postmortem Brain Slices to MRI Reference Volume"*, IEEE Trans. Nucl. Sci., Vol. 47, No. 4, pp. 1607-1613, 2000.

[22] T.-S. Kim, R. E. N, Shehada, and V. Z. Marmarelis, *"Nonlinear modeling of ultrasound transmit-receive system using Laguerre-Volterra networks"*, Proc. SPIE Medical Imaging, Vol. 5035, pp. 62-69, 2003.